L-390

NATIONAL ADVISORY COMMITTEE FOR AERONAUTICS

WARTIME REPORT

ORIGINALLY ISSUED
December 1943 as
Advance Confidential Report 3L03

A COMPARISON AT HIGH SPEED OF THE AERODYNAMIC MERITS

OF MODELS OF MEDIUM BOMBERS HAVING THICKENED

WING ROOTS AND HAVING WINGS WITH NACELLES

By Eugene C. Draley

Langley Memorial Aeronautical Laboratory
Langley Field, Va.

NACA

WASHINGTON

NATIONAL ADVISORY COMMITTEE FOR AERONAUTICS

ADVANCE CONFIDENTIAL REPORT

A COMPARISON AT HIGH SPEED OF THE AERODYNAMIC MERITS

OF MODELS OF MEDIUM BOMBERS HAVING THICKENED
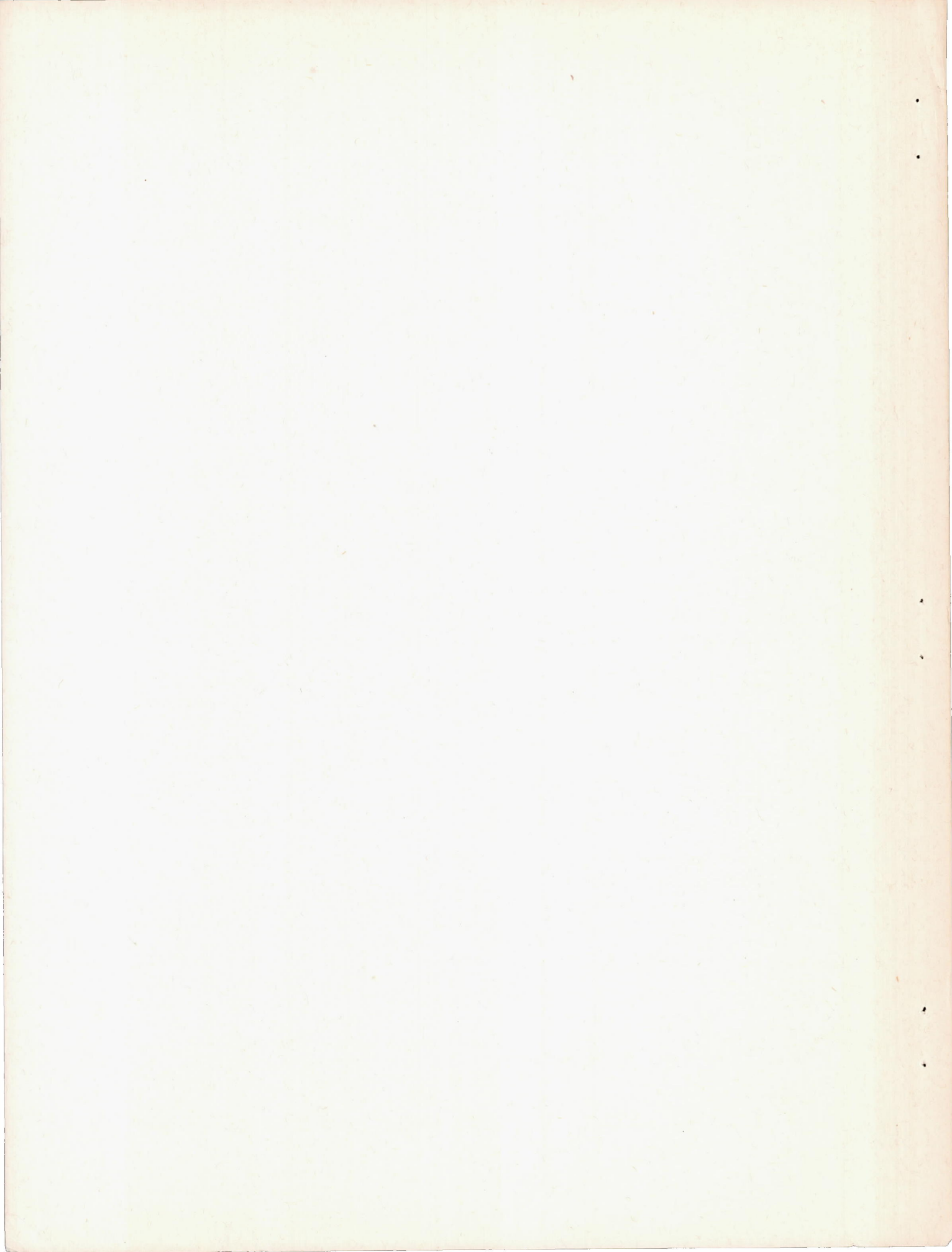
WING ROOTS AND HAVING WINGS WITH NACELLES

By Eugene C. Draley

SUMMARY

Models of medium-bomber designs of the Army Air Forces, Materiel Command, were tested in the NACA 8-foot high-speed tunnel to investigate the relative characteristics of thickened wing roots with propeller-shaft fairings and wings with nacelles. The effect of nacelle vertical location was also investigated.

Incremental drag coefficients due to thickened wing roots and due to propeller-shaft fairings are presented through a Mach number range up to 0.70 at a lift coefficient of 0.10. Pressure measurements at each wing-fuselage juncture tested at Mach numbers up to about 0.60 are also presented for a lift coefficient of 0.10.

Increasing the thickness ratio of a wing-fuselage juncture from 16.9 percent to 22.2 percent caused an increment in airplane drag coefficient of 0.0005 at a Mach number of 0.60 and caused a reduction in critical speed. With a wing-fuselage section thickened the same amount but with the thickness ratio held the same by the use of fillets extending the wing chord, this drag increment was reduced about 50 percent and large increases in critical speed were obtained. Large nacelle drags and low critical speeds were measured with nacelles in a low position with respect to the wing. The designs with thickened wing roots and propeller-shaft fairings had important improvements in both drag and critical speed as compared with the designs including the more conventional engine-nacelle installation. With improper air inlets, however, the probable gain may be nullified.

INTRODUCTION

In the design of multiengine airplanes, large savings in nacelle drags are indicated if engines of the same horsepower can be completely submerged in the wing or fuselage and the propellers can be driven through a drive-shaft arrangement with a small fairing around the propeller shaft. The design with the engines in the fuselage would, however, entail mechanical and arrangement difficulties. A compromise design would be one in which the engines are completely submerged in the wing roots. In very large airplanes, this type of installation may be possible without thickening the wing roots but, in medium-size airplanes, thickening of the wing roots would be required to permit a satisfactory engine installation. This problem becomes one of determining the merits of thickened wing roots and propeller-shaft fairings as compared with a conventional nacelle installation.

Discussion of this problem by representatives of the Army Air Forces and the National Advisory Committee for Aeronautics led to a request by the Army Air Forces for tests of models incorporating features that would permit comparison of thickened wing roots with propeller-shaft fairings and wings with nacelles. These models were accordingly constructed and tested in the NACA 8-foot high-speed tunnel at the Langley Memorial Aeronautical Laboratory. This report presents an analysis of the most important results obtained in the investigation requested by the Army Air Forces.

Measurements of forces were made at speeds corresponding to Mach numbers as high as 0.70. Measurements of wing-fuselage juncture pressures were made at Mach numbers up to about 0.60.

APPARATUS AND METHODS

The tests were conducted in the NACA 8-foot high-speed tunnel. This tunnel is a single-return, closed-throat type with a circular cross section. The residual air-stream turbulence is very low but is somewhat greater than that of free air.

The models were proportioned to correspond to a $\frac{1}{7}$-scale model of a medium-size, two-engine bomber design. The wing tips were not reproduced and all the model configurations were so mounted that the wings completely spanned the test section (figs. 1 to 4); the wings passed through cut-outs in the tunnel walls to the balance ring.

Four wings were tested. Each wing is designated by the numerals of the NACA airfoil section at or near the wing root. The symmetrical 0017-34 wing and the cambered 450-217 wing were basic wings representing designs in which the wing roots were of the usual thickness ratios. The symmetrical 0024-34 wing and the cambered 450-117 wing were modifications of the 0017-34 wing and the 450-217 wing, respectively, in which the wing roots were thickened in order to permit submerged-engine installations at the wing roots. (See figs. 1 to 4.) It should be noted that, because of the sharp thickness-ratio taper of the 0024-34 wing, the thickness ratio of this wing at the fuselage juncture was 0.222.

The 0017-34 wing had an NACA 0017-34 root section (at the wing center line) and tapered to an NACA 0013.1-34 profile at the tunnel walls. This wing had 1.7° washout. (See fig. 1.) The ordinates for three sections of this wing are presented in table I.

The 0024-34 wing was identical with the 0017-34 wing outboard of a station 19.143 inches from the wing center line. Inboard of this station, the absolute thickness was increased linearly with the result that the wing root was an NACA 0024-34 airfoil section. The plan form and washout were unchanged. (See fig. 1 and table I.)

The 450-217 wing had an NACA 450-217 root section and an NACA 450-(0.3)(13.1) section at the tunnel wall; this wing therefore had the same spanwise thickness-ratio variation and the same plan form as the 0017-34 wing. The 450-217 wing had no geometrical washout but the camber variation was so adjusted that the lift at each section would correspond to the values for the 0017-34 wing at the high-speed attitude. (See figs. 2 to 4 and table II.)

The root section of the 450-217 wing was thickened to give the 450-117 wing, which had the same absolute

thickness variation as the 0024-34 wing.   The chord near
the fuselage of the 450-117 wing, however, was increased
by filleting to reduce the thickness ratio to 17 percent.
(See fig. 1 and table II.)   This increase in chord also
required a reduction of the camber for the increased-
chord sections to retain the same spanwise lift loading
at the high-speed attitude as for the other wings.

In order to simulate fuselage interference effects,
all configurations included the fuselage shown in fig-
ures 1 to 4.   The fuselage was provided with a set of
removable blocks to accommodate in a midwing position
each of the four wings.   These blocks were arranged to
set the angle of incidence with respect to the fuselage
reference line at 2° for the symmetrical wings and at 0°
for the cambered wings.   The horizontal tail surfaces
were omitted because these components have no significant
effects on the problem under investigation.

The propeller-shaft fairings, representing a covering
for the propeller shafts in the submerged-engine designs,
were bodies of revolution with the axis located
19.143 inches from the wing center line.   (See figs. 1
and 3.)   The angle of incidence of the propeller-shaft
fairings was 0° with respect to the fuselage reference
line in all test configurations.

The nacelles representing the conventional engine-
nacelle installations were elliptical in cross section
and were 1.47 times the wing chord in length.   (See
figs. 2 and 4.)   Actually only one nacelle shape was
investigated but two sets of nacelles were tested.   The
first set was tested in a midwing position; the nacelle
center line was coincident with the wing chord.   The
second set of nacelles was tested in a low position so
arranged that the upper profile of the nacelles faired
into the wing upper surface at the point of maximum
thickness.   This vertical displacement located the
nacelle center line about 10 percent of the wing chord
below the wing chord line.

The propeller-shaft fairings were tested on the
0017-34, the 0024-34 (thickened 0017-34), and the
450-117 (filleted 450-217) wings.   The nacelles were
tested on only the 450-217 wing.   All test configura-
tions are represented in figures 3 and 4.   In order to
evaluate the characteristics of the nacelles and propeller-
shaft fairings, tests of all the wing-fuselage combinations

L-390

represented were made with and without the nacelles and propeller-shaft fairings. No tests were made with the propellers on the model and no provisions for engine-cooling-air flow were made for any of the models tested.

Force measurements were made through a range of Mach number as high as 0.70 at angles of attack covering lift coefficients greater than and less than 0.10. Pressure-distribution measurements for the wing-fuselage juncture are presented for a similar range of angle of attack for Mach numbers as high as approximately 0.60. Pressure measurements at the wing-nacelle junctures were not made.

Transition was fixed on all the test configurations by a $\frac{1}{4}$-inch strip of carborundum grains shellacked to the surface of the models (figs. 3 and 4). Transition was fixed at 10 percent of the chord on both the upper and the lower surfaces of all wings and on the fuselage at a station 10 percent of the fuselage length behind the nose. On the nacelles and propeller-shaft fairings, the carborundum strip was located at the plane of the propellers.

RESULTS

All the data presented herein are in nondimensional form based on free-stream dynamic pressure

$$q = \frac{1}{2}\rho V^2$$

where

ρ mass density of air, slugs per cubic foot

V free-stream velocity, feet per second

The incremental drag coefficients and lift coefficients are based on a wing area of 12.25 square feet. All the data have been cross-plotted to obtain data at a constant lift coefficient of 0.10. The angle of attack α is measured from the fuselage reference line.

None of the results herein presented have been corrected for tunnel-wall effects or buoyancy effects. Because of the smallness of the models, however, neither of these corrections to drag or pressures is large for the complete models; these corrections will be insignificant for the propeller-shaft fairings, nacelles, and thickened wing roots and therefore will not affect comparisons of these components.

Force Tests

In order to evaluate the effect on drag of thickening the 0017-34 wing, the differences between the drag coefficients for the wing-fuselage configuration with the 0017-34 wing and with the 0024-34 wing were obtained. These differences are plotted in figure 5 as incremental drag coefficient ΔC_D against Mach number M at a lift coefficient C_L of 0.10. Similarly, the effect of thickening and filleting was obtained from the difference between the wing-fuselage configuration with the 450-217 wing and with the 450-117 wing. Also included in figure 5 are the incremental drag coefficients due to the propeller-shaft fairings tested on configurations shown in figure 3. These increments were obtained as the differences in drag coefficients with and without the propeller-shaft fairings for each of the three configurations involving the 0017-34 wing, the 0024-34 wing, and the 450-117 wing. The incremental drag coefficients thus obtained were so nearly identical for each of the three configurations that they are represented by one curve. The incremental drag coefficients for the nacelles on the 450-217 wing were also obtained from the differences in drag coefficients of the test configurations with and without the nacelles.

In evaluating the drag of a submerged-engine installation, both the drag of the propeller-shaft fairings and the drag of the thickened wing root should be included. The incremental drag coefficients due to the thickened wing root of the 0017-34 wing (fig. 5) were therefore added to the incremental drag coefficients of the propeller-shaft fairings. The results are plotted in figure 6 and are shown in table III. The drag coefficients chargeable to a submerged-engine installation with a filleted wing root were similarly obtained by adding the incremental drag coefficients of the thickened and filleted wing root of the 450-217 wing to the incremental drag

coefficients of the propeller-shaft fairings and are presented in figure 6. Also included for comparison are the incremental drag coefficients of the midnacelles and low nacelles.

In order to illustrate the effect on lift of nacelle vertical location, figure 7 presents lift coefficient plotted against angle of attack at a Mach number of 0.50 for the 450-217 wing and fuselage alone, with the midnacelles, and with the low nacelles.

Pressure-Distribution Tests

The results of the pressure measurements at the wing-fuselage junctures of all the configurations are presented in figure 8 in terms of pressure coefficient P, where

$$P = \frac{\text{Local static pressure} - \text{Free-stream static pressure}}{\text{Free-stream dynamic pressure}}$$

Figures 8(a) to 8(c) are representative of the wing-fuselage configurations with the propeller-shaft fairings because no measurable changes in the pressures over the wing-fuselage juncture were noted when the propeller-shaft fairings were added.

The peak pressure coefficients for each of the configurations represented in figure 8 are plotted against Mach number in figure 9. Each of these variations is extrapolated to the critical pressure coefficient P_{cr}, which is the pressure coefficient corresponding to the local speed of sound. In making these extrapolations, the general trend of the pressure-coefficient variation with Mach number given by Temple and Yarwood (reference 1) and a few isolated test points were used as a guide. The intersection of the peak pressure coefficient with the P_{cr}-line is therefore the critical speed of the configuration. (See table III.)

DISCUSSION

Effect of Thickening and Filleting

Increasing the thickness ratio of the 0017-34 wing root from 17 percent to 24 percent led to an incremental

drag coefficient of 0.0005 at a Mach number of 0.60 (fig. 5). Only the root section of the 0024-34 wing was 24-percent thick and the exposed section at the wing-fuselage juncture was considerably less; the increment in drag therefore represents a change in thickness ratio at the wing-fuselage juncture from 16.9 percent to 22.2 percent.

With further increases in Mach number, the rather sharp increases in drag coefficient are undoubtedly due to the early onset of serious compressibility effects for the thickened wing. The critical Mach number was reduced from 0.71 to 0.70 (fig. 9). This change in critical speed is rather small for a change in thickness ratio from 16.9 percent to 22.2 percent. The spanwise thickness-ratio taper is unusually sharp, however, with the result that significant departures from an ideal two-dimensional flow over these sections must undoubtedly have occurred.

Such relatively small increases in drag at subcritical speeds and reductions in critical speed which must be associated with the extreme thickness-ratio taper appear to indicate that, in such designs, the wing root may be thickened with considerably smaller detrimental effects than would at first be estimated on the basis of two-dimensional assumptions. At increased lift coefficients and Mach numbers, however, the drag may be considerably increased because of more serious compressibility effects leading to separation on the thickened portion of the wing. It has been shown that recent NACA low-drag airfoils with thickness ratios much greater than 18 percent may be susceptible to increases in drag due to separation (reference 2). Although the favorable effect of small spanwise flow that may be associated with the high local thickness-ratio taper is indicated, careful consideration and further investigation would be required before this effect could be fully realized in a particular design.

With the same amount of thickening but with the wing-fuselage sections kept 17-percent thick by use of fillets, the drag increment for the 450-217 wing-fuselage section with fillets is 0.0002, which is about one-half the value for the thickened 0017-34 wing (fig. 5). The filleting was not so extensive as it should have been. The thickening was started at the propeller-shaft-fairing station and increased inboard (fig. 1). The filleting,

however, was not extended outboard to the propeller-shaft fairings. The result was that sections immediately outboard of the fillets were 19-percent thick. These thicker sections probably lead to somewhat greater drag increments than would result if the filleting were such that a continuously decreasing thickness-ratio taper was maintained (Mach numbers above 0.60, fig. 5).

The critical speed of the filleted wing-fuselage juncture was the highest of the test configurations, with a critical Mach number of 0.73. This value represents an increase in critical Mach number from 0.71 to 0.73 due to the effect of the fillets, even though the 450-217 wing and the 450-117 wing had the same thickness ratio. This increase in critical speed is largely due to the reduction in root section lift coefficient for the same over-all lift coefficients permitted by the additional wing area of the fillets.

Nacelles and Propeller-Shaft Fairings

Although the drag increment of the propeller-shaft fairings is only about 20 percent of the drag increment of the midnacelles at a Mach number of 0.60, even greater differences are indicated at higher speeds as the drag of the midnacelles is further increased by compressibility effects. It should be noted, however, that at a Mach number of 0.60 the drag coefficient, based on frontal area, of the midnacelles is 0.0262 as compared with 0.0375 for the propeller-shaft fairings. The drag coefficient of the midnacelles thus is of the same order as that for the propeller-shaft fairings. The difference in drag force at subcritical speeds is almost entirely due to the difference in size of the two bodies.

In addition to the smaller drag of the propeller-shaft fairings resulting from the smaller size as compared with the midnacelles, the propeller-shaft fairings led to no changes in the critical speed of the wing-fuselage junctures; whereas the midnacelles led to a reduction of approximately 0.03 in critical Mach number. (See fig. 9.) This difference corresponds to 21 miles per hour at an altitude of 25,000 feet.

A further reduction in the over-all critical speed of the configuration can be expected from the nacelle

interference. An indication of this effect is shown in figure 5 in which, for the midnacelles, an appreciable increase of the drag coefficient is evident at Mach numbers less than the critical value for the wing-fuselage juncture.

When the same nacelle was tested in the low position, the nacelle drag was about doubled at low speeds and increased even more at high speeds (fig. 5). Unpublished data from several tests of different nacelles in a low position have shown that, in this location, the nacelles cause important increases in the average local velocities over the lower surface of the wing-nacelle junctures. Such increases in local velocities lead to increased pressure-recovery gradients, which cause separation. With increases in speed, the separation is further aggravated by compressibility effects (see reference 3) and therefore can account for the rise in the drag coefficient with Mach number.

A further important effect of the low nacelles is the large loss in lift caused by the increased lower-surface velocities. At the same angle of attack, large reductions in lift coefficient are noted for the configuration including the nacelles in the low position (fig. 7). This change requires an increase in angle of attack of about 1° to maintain the same lift coefficient, which is the basis of comparison used in the present investigation. Such a change leads to an irregular spanwise lift loading that requires more lift to be carried on the wing root and tip sections. Comparisons of the pressure distributions at the wing-fuselage juncture for the 450-217 wing and fuselage and for the 450-217 wing with fuselage and low nacelles indicate that, for the same over-all wing lift coefficient, the wing-fuselage juncture appears to be carrying a greater lift load, particularly near the leading edge, with the low-nacelle configuration (figs. 8(c) and 8(f)).

Such effects will lead not only to increases in wing drag but also to a reduction in critical speed. The critical Mach number of the wing-fuselage juncture for the configuration with the low nacelles is 0.66 as compared with 0.71 for the wing-fuselage combination alone and 0.68 for the wing with fuselage and midnacelles. The nacelles in the low position therefore lead to a reduction in critical speed of 35 miles per hour at 25,000 feet. When compared with the reduction in

critical speed of 21 miles per hour for the midnacelles, this value of critical speed indicates that a reduction in critical speed of 14 miles per hour is chargeable only to the location of the nacelle.

Comparison of Submerged Engines and

Engine-Nacelle Combinations

The submerged-engine configurations generally have considerably lower drag and higher critical speeds than the conventional engine-nacelle arrangements (fig.6 and table III). Although the configuration of the 0017-34 wing with fuselage and propeller-shaft fairings has the lowest incremental drag coefficients due to an engine installation, $\Delta C_D = 0.0003$, such a design may prove impracticable for medium-size airplanes because the engines would have to be in the fuselage and would involve mechanical and arrangement complications. The configuration that has both low drag and the highest critical speed of the combinations tested is the 450-117 wing (filleted 450-217) with propeller-shaft fairings. The incremental drag coefficient chargeable to the submerged-engine installation is only 0.0005 for this configuration and further reductions by more extensive filleting are indicated. The wing-fuselage critical Mach number of this combination, moreover, is 0.73 as compared with 0.71 for the 0017-34 wing configuration. The configuration of the 0024-34 wing with fuselage and propeller-shaft fairings has a somewhat greater incremental drag coefficient due to the submerged-engine installation of 0.0008 and a considerably lower critical speed (critical Mach number $M_{cr} = 0.70$) than the filleted configuration.

The incremental drag of the configuration of the 450-217 wing with fuselage and midnacelles is lower than the incremental drag of the configurations with the low nacelles. The incremental drag coefficient chargeable to the engine installation for this configuration is 0.0015 (fig. 6), which is three times the value for the submerged-engine configuration with filleting (table III). The critical Mach number is only 0.68 as compared with 0.73 for the filleted configuration. This difference represents a difference in speed of 35 miles per hour at 25,000 feet.

The configuration having the greatest drag and the lowest critical speed consists of the 450-217 wing with fuselage and low nacelles. The incremental drag coefficient chargeable to the engine installation (at a Mach number of 0.60) for this configuration is about three times the value for the same configuration with mid-nacelles. The critical Mach number for the configuration with low nacelles is further reduced to 0.66.

The results of this investigation relate solely to the external flow over the wings and bodies. Although it is indicated that wing roots thickened to house engine installations show advantage, the possible gain could be nullified by improper air-inlet installations. A considerable amount of research may be necessary to develop proper inlets in the swept-back portion of the wing leading edge in order to realize the probable advantage indicated.

CONCLUSIONS

The results of the high-speed tests of models of medium bombers have indicated the following conclusions:

1. Increasing the thickness ratio of a wing-fuselage juncture from 16.9 percent to 22.2 percent led to an increment in airplane drag coefficient of 0.0005 at a Mach number of 0.60 and a reduction in the critical Mach number from 0.71 to 0.70.

2. Thickening a wing-fuselage juncture but maintaining the same thickness ratio by increasing the chord in the form of fillets caused an increment in airplane drag coefficient of 0.0002 and led to an increase in critical Mach number for the wing-fuselage juncture of from 0.71 to 0.73.

3. Large increases in nacelle drag and reductions in critical speed were measured when the nacelle was in a low position with respect to the wing.

4. The submerged-engine designs had lower drag and higher critical speeds than the conventional engine-nacelle designs tested. The best engine-nacelle design caused an increment in airplane drag coefficient,

L-390

chargeable to the engine-nacelle installation, that was
about three times the corresponding value for the best
practicable submerged-engine design. At the same time,
the critical Mach number of the wing-fuselage juncture
of the engine-nacelle configuration was 0.68 as com-
pared with the corresponding value of 0.73 for the
submerged-engine design. With improper air inlets,
however, the probable gains indicated may be nullified.

Langley Memorial Aeronautical Laboratory,
        National Advisory Committee for Aeronautics,
            Langley Field, Va.

REFERENCES

1. Temple, G., and Yarwood, J.: The Approximate Solu-
        tion of the Hodograph Equations for Compressible
        Flow. Rep. No. S.M.E. 3201, R.A.E., June 1942.

2. Jacobs, Eastman N., Abbott, Ira H., and Davidson,
        Milton: Investigation of Extreme Leading-Edge
        Roughness on Thick Low-Drag Airfoils to Indicate
        Those Critical to Separation. NACA C.B., June
        1942.

3. Stack, John: Compressibility Effects in Aeronautical
        Engineering. NACA A.C.R., Aug. 1941.

TABLE I.- PROFILE ORDINATES FOR SYMMETRICAL WINGS

[Stations and ordinates are in inches]

0017-34 wing; section at wing center line		0024-34 wing; section at wing center line		0017-34 wing and 0024-34 wing			
				Section 19.143 in. from wing center line		Section 41 in. from wing center line	
Station	Ordinate	Station	Ordinate	Station	Ordinate	Station	Ordinate
0	0	0	0	0	0	0	0
.309	.397	.309	.560	.238	.284	.309	.560
.618	.588	.618	.830	.476	.421	.618	.830
1.236	.837	1.236	1.232	.952	.625	1.236	1.232
1.854	1.097	1.854	1.549	1.428	.736	1.854	1.549
2.471	1.279	2.471	1.806	1.903	.916	2.471	1.806
3.707	1.573	3.707	2.221	2.855	1.127	3.707	2.221
4.943	1.783	4.943	2.518	3.807	1.277	4.943	2.518
7.414	2.031	7.414	2.867	5.711	1.454	7.414	2.867
9.886	2.101	9.886	2.966	7.614	1.504	9.886	2.966
12.357	2.040	12.357	2.880	9.518	1.461	12.357	2.880
14.828	1.863	14.828	2.630	11.421	1.334	14.828	2.630
17.300	1.569	17.300	2.214	13.325	1.123	17.300	2.214
19.771	1.162	19.771	1.641	15.229	.832	19.771	1.641
22.243	.654	22.243	.923	17.132	.468	22.243	.923
23.478	.359	23.478	.507	18.084	.257	23.478	.507
24.714	.042	24.714	.059	19.035	.030	24.714	.059

TABLE II.- PROFILE ORDINATES FOR CAMBERED WINGS

[Stations and ordinates are in inches]

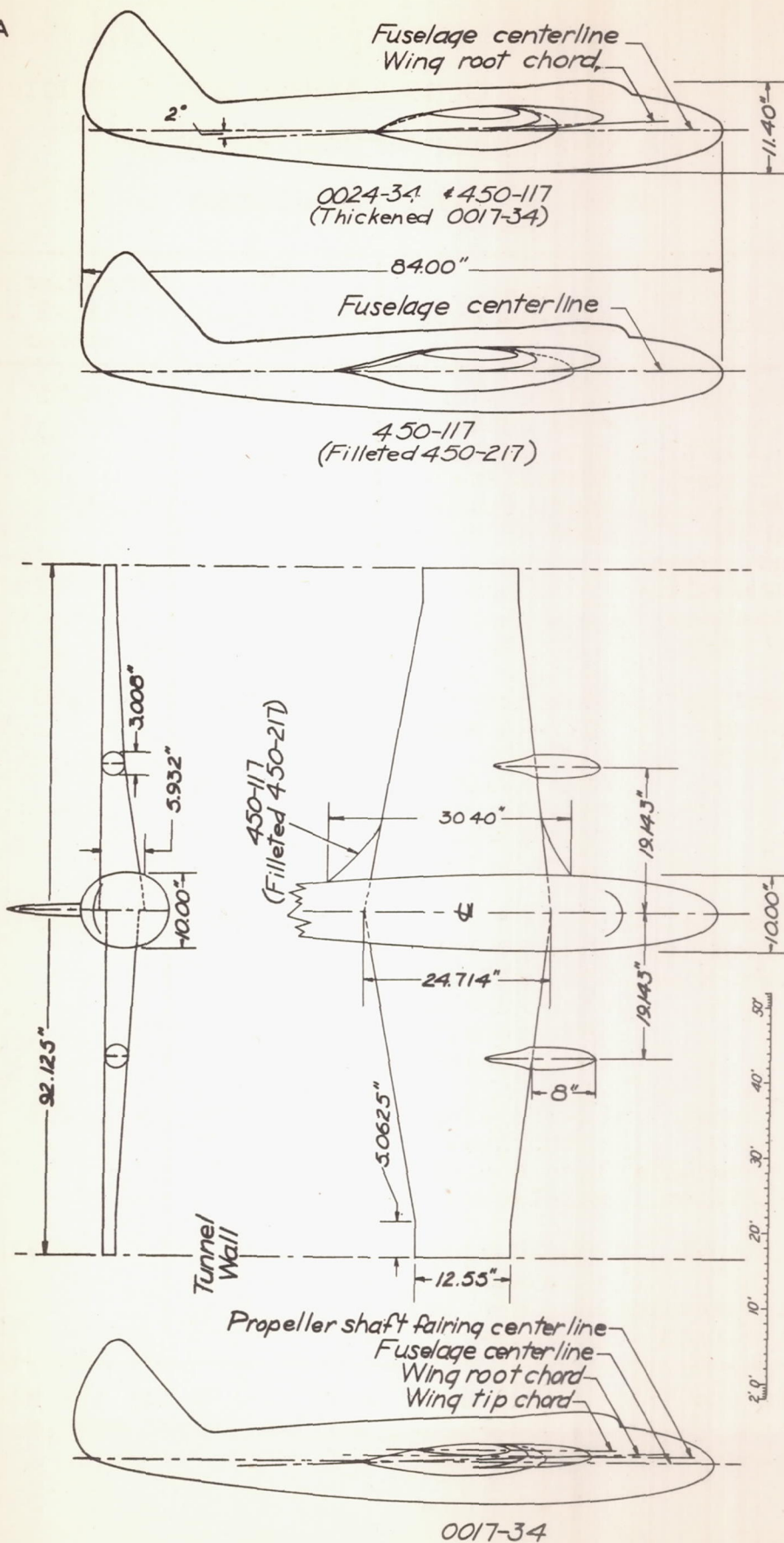| 450-217 wing; section at wing center line				450-117 wing; section 5.0 in. from wing center line				450-217 wing and 450-117 wing							
								Section 19.143 in. from wing center line				Section 41 in. from wing center line			
Upper surface		Lower surface		Upper surface		Lower surface		Upper surface		Lower surface		Upper surface		Lower surface	
Station	Ordinate	Station	Ordinate	Station	Ordinate	Station	Ordinate	Station	Ordinate	Station	Ordinate	Station	Ordinate	Station	Ordinate
0	0	0	0	0	0	0	0	0	0	0	0	0	0	0	0
.277	.595	.341	.552	.353	.724	.407	.688	.224	.421	.252	.401	.154	.228	.160	.222
.581	.826	.655	.752	.729	1.002	.791	.940	.459	.583	.492	.548	.310	.315	.318	.305
1.195	1.139	1.276	1.014	1.486	1.378	1.554	1.272	.934	.802	.970	.742	.623	.431	.632	.414
1.812	1.372	1.895	1.204	2.245	1.656	2.315	1.514	1.409	.963	1.446	.882	.937	.516	.946	.494
2.431	1.555	2.512	1.350	3.006	1.873	3.074	1.701	1.885	1.090	1.922	.991	1.251	.583	1.259	.556
3.670	1.822	3.744	1.556	4.528	2.191	4.592	1.966	2.838	1.274	2.872	1.146	1.879	.680	1.886	.645
4.910	2.003	4.975	1.688	6.052	2.404	6.108	2.137	3.792	1.398	3.822	1.247	2.507	.744	2.513	.703
7.392	2.229	7.436	1.844	9.101	2.668	9.139	2.343	5.701	1.551	5.720	1.366	3.763	.824	3.767	.773
9.875	2.312	9.896	1.889	12.151	2.763	12.169	2.405	7.609	1.607	7.619	1.403	5.019	.852	5.021	.795
12.357	2.230	12.357	1.794	15.200	2.660	15.200	2.291	9.518	1.547	9.518	1.336	6.275	.818	6.275	.760
14.837	1.941	14.820	1.517	18.248	2.306	18.232	1.947	11.425	1.340	11.417	1.136	7.531	.706	7.529	.649
17.314	1.501	17.286	1.116	21.292	1.772	21.268	1.447	13.331	1.030	13.318	.845	8.787	.538	8.783	.487
19.786	.963	19.757	.648	24.332	1.125	24.308	.858	15.234	.653	15.222	.502	10.042	.337	10.038	.295
22.251	.410	22.234	.205	27.367	.465	27.353	.292	17.135	.269	17.128	.171	11.296	.134	11.294	.107
23.483	.174	23.474	.049	28.884	.190	28.876	.085	18.085	.110	18.081	.050	11.923	.052	11.922	.036
24.714	0	24.714	0	30.400	0	30.400	0	19.035	0	19.035	0	12.550	0	12.550	0

TABLE III.- COMPARISONS OF INCREMENTAL DRAG COEFFICIENTS

AND WING-FUSELAGE CRITICAL SPEEDS OF

TYPES OF ENGINE INSTALLATION

Type of engine installation	Test configuration	ΔC_D at M = 0.60 (1)	Wing-fuselage critical Mach number
In fuselage with long drive shaft or with engine submerged in wing of large airplane without thickening of wing	0017-34 wing with fuselage and propeller-shaft fairings	0.0003	0.71
Submerged in thickened wing root	Thickened 0017-34 wing (0024-34 wing) with fuselage and propeller-shaft fairings	.0008	.70
Submerged in thickened and filleted wing root	Filleted 450-217 wing (450-117 wing) with fuselage and propeller-shaft fairings	.0005	.73
Conventional midwing engine-nacelle installation	450-217 wing with fuselage and mid-nacelles	.0015	.68
Conventional low-wing engine-nacelle installation	450-217 wing with fuselage and low nacelles	.0045	.66

[1]Values are incremental drag coefficients for all components given in test-configuration column except fuselage and original wing.

Fig. 1

Fuselage centerline
Wing root chord

2°

1.40"

0024-34 ¢450-117
(Thickened 0017-34)

84.00"

Fuselage centerline

450-117
(Filleted 450-217)

NATIONAL ADVISORY
COMMITTEE FOR AERONAUTICS

Tunnel
Wall

.3.008"

5.932"

10.00"

450-117
(Filleted 450-217)

30.40"

19.143"

24.714"

10.00"

19.143"

92.125"

5.0625"

8"

12.55"

50'

40'

30'

20'

Propeller shaft fairing centerline
Fuselage centerline
Wing root chord
Wing tip chord

10'

2',0'

0017-34

Figure 1.—Test model configurations for the 0017-34, 450-117(Filleted 450-217),
and 0024-34(Thickened 0017-34) wings.

NACA

Fig. 2

L-390

Wing root chord and fuselage centerline
Nacelle station wing chord and nacelle centerline
Wing tip chord

Root chord NACA 450-217

7.00"
.920"

24.714"
19.143"

19.035"
19.143"

92.125"

.50625"

28"

Tunnel Wall

12.55"

Nacelle centerline
Wing root chord and fuselage centerline
Nacelle station wing chord

1.89"

2'.0"   10'   20'   30'   40'   50'
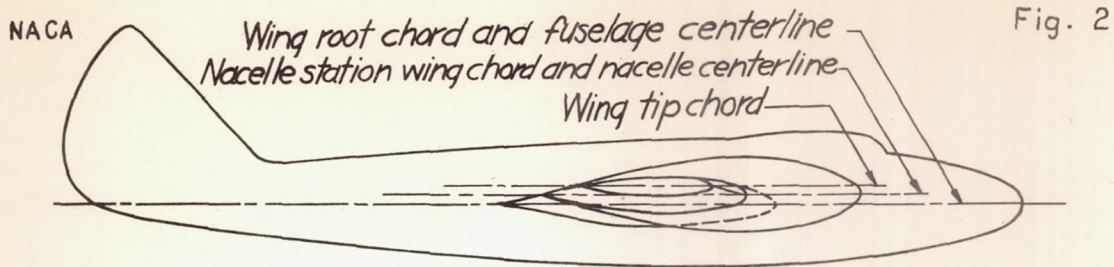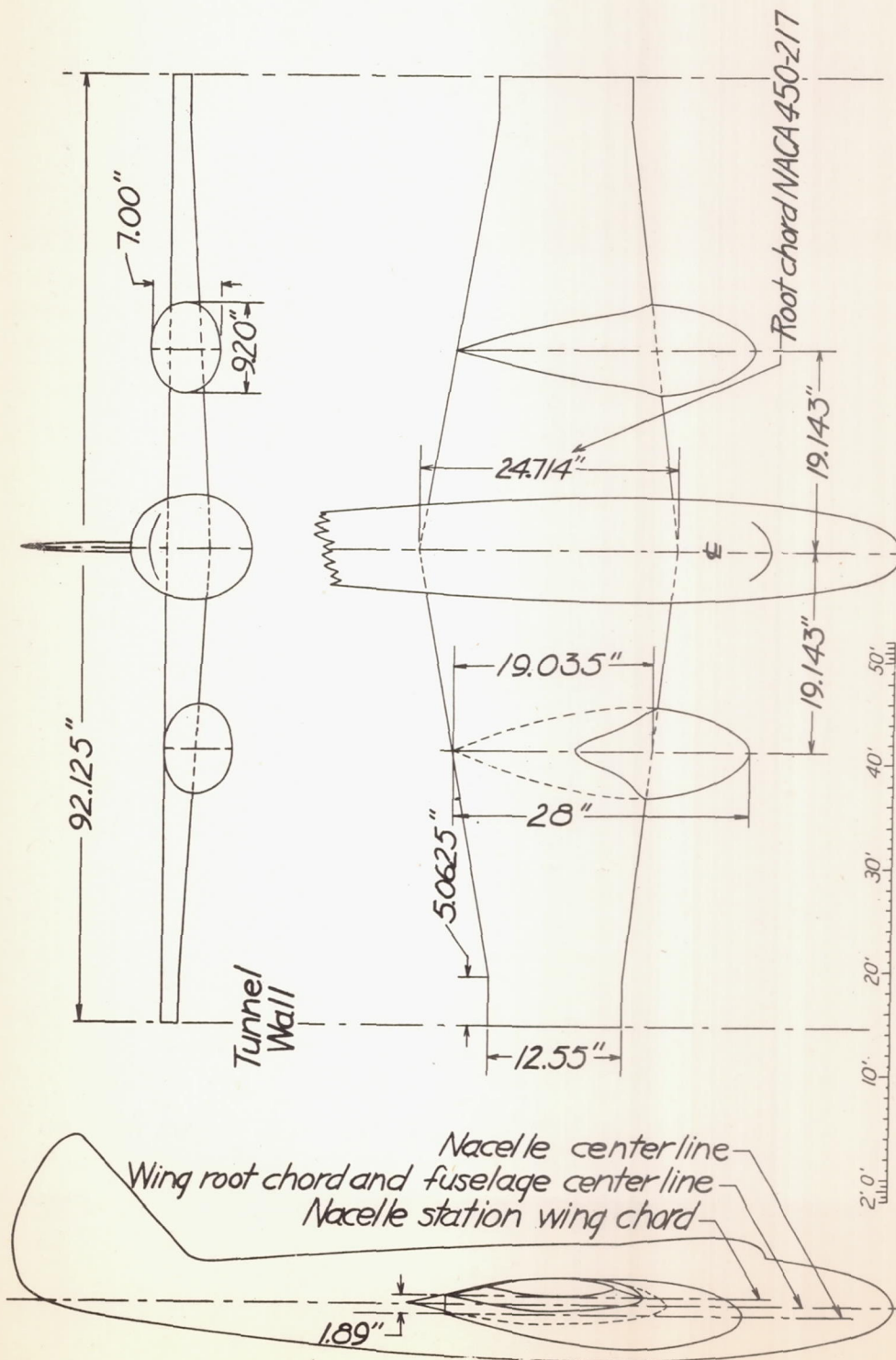
Figure 2. — Test model configurations for the   450-217 wing.
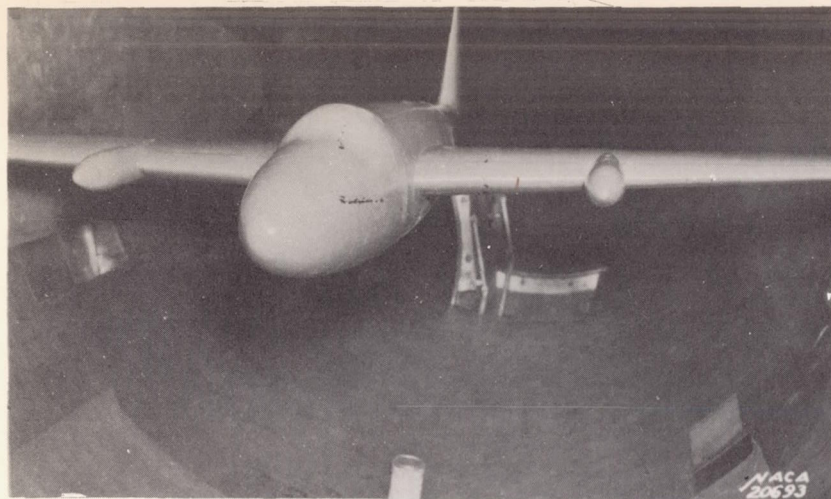
(a) 0017-34 wing.
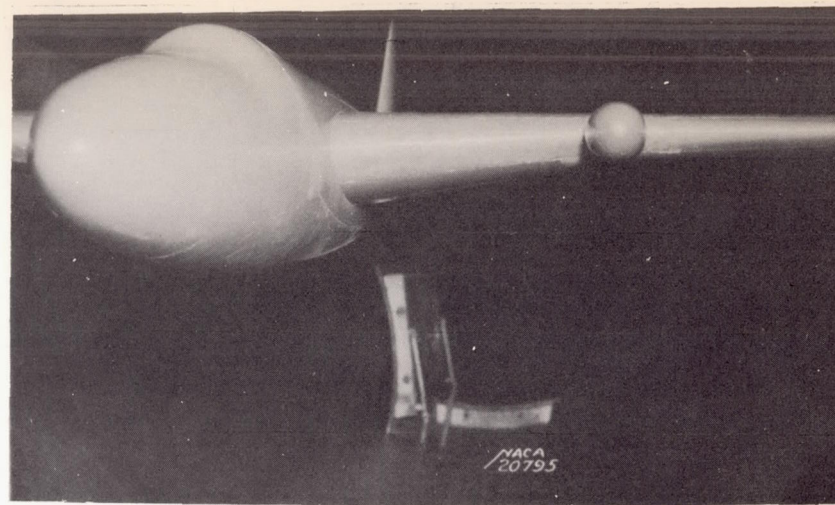
(b) 0024-34 wing (thickened 0017-34 wing).

(c) 450-117 wing (filleted 450-217 wing).

Figure 3.- Test configurations for the 0017-34 wing, the 0024-34 wing, and the 450-117 wing.

Fig. 3
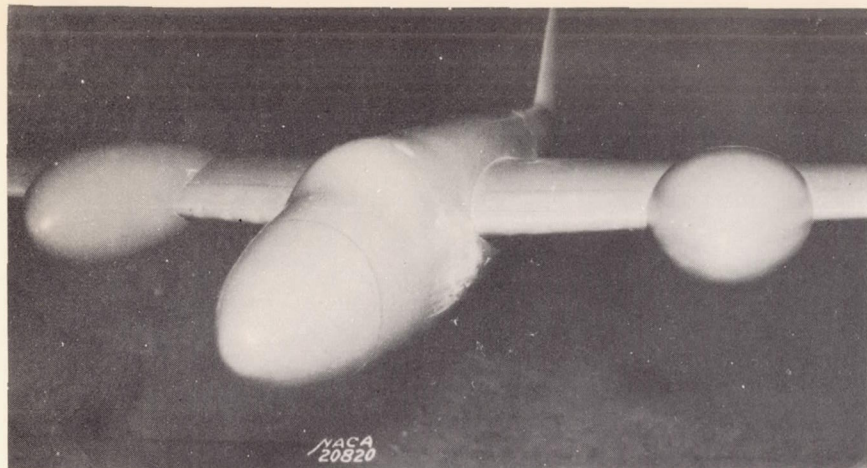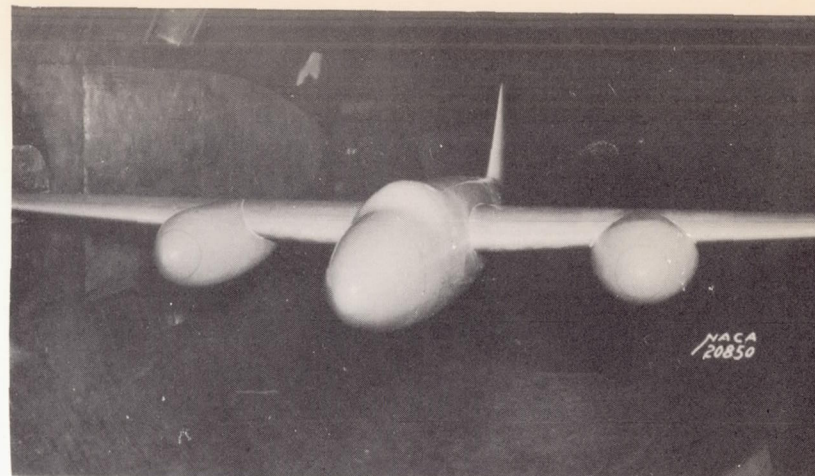
(a) Midnacelles.

(b) Low nacelles, front view.
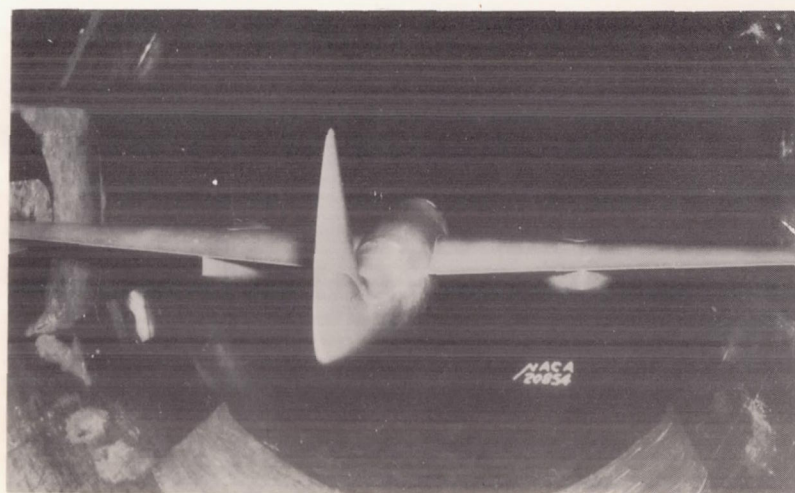
(c) Low nacelles, rear view.

Figure 4.- Test configurations with 450-217 wing.

Fig. 4
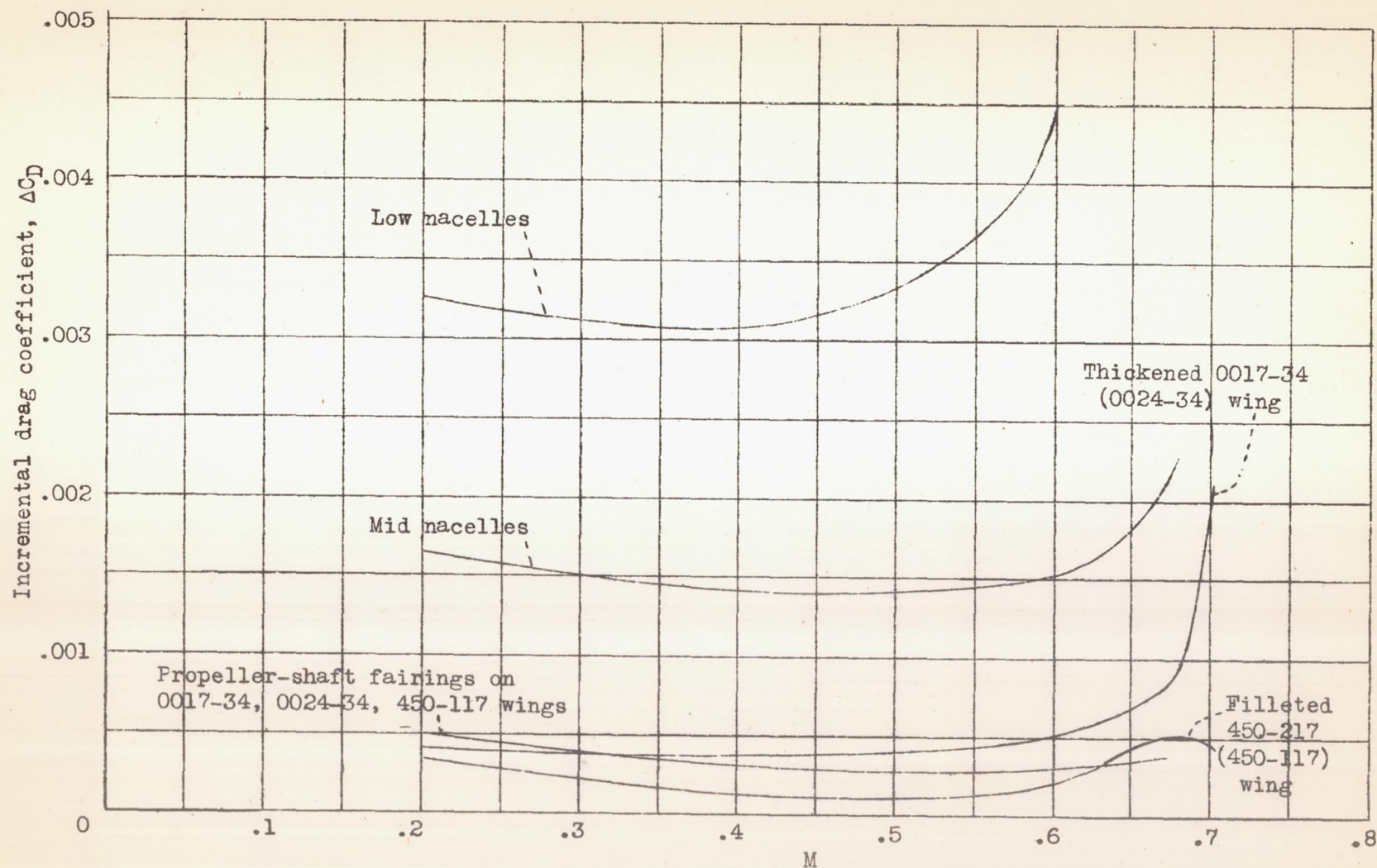
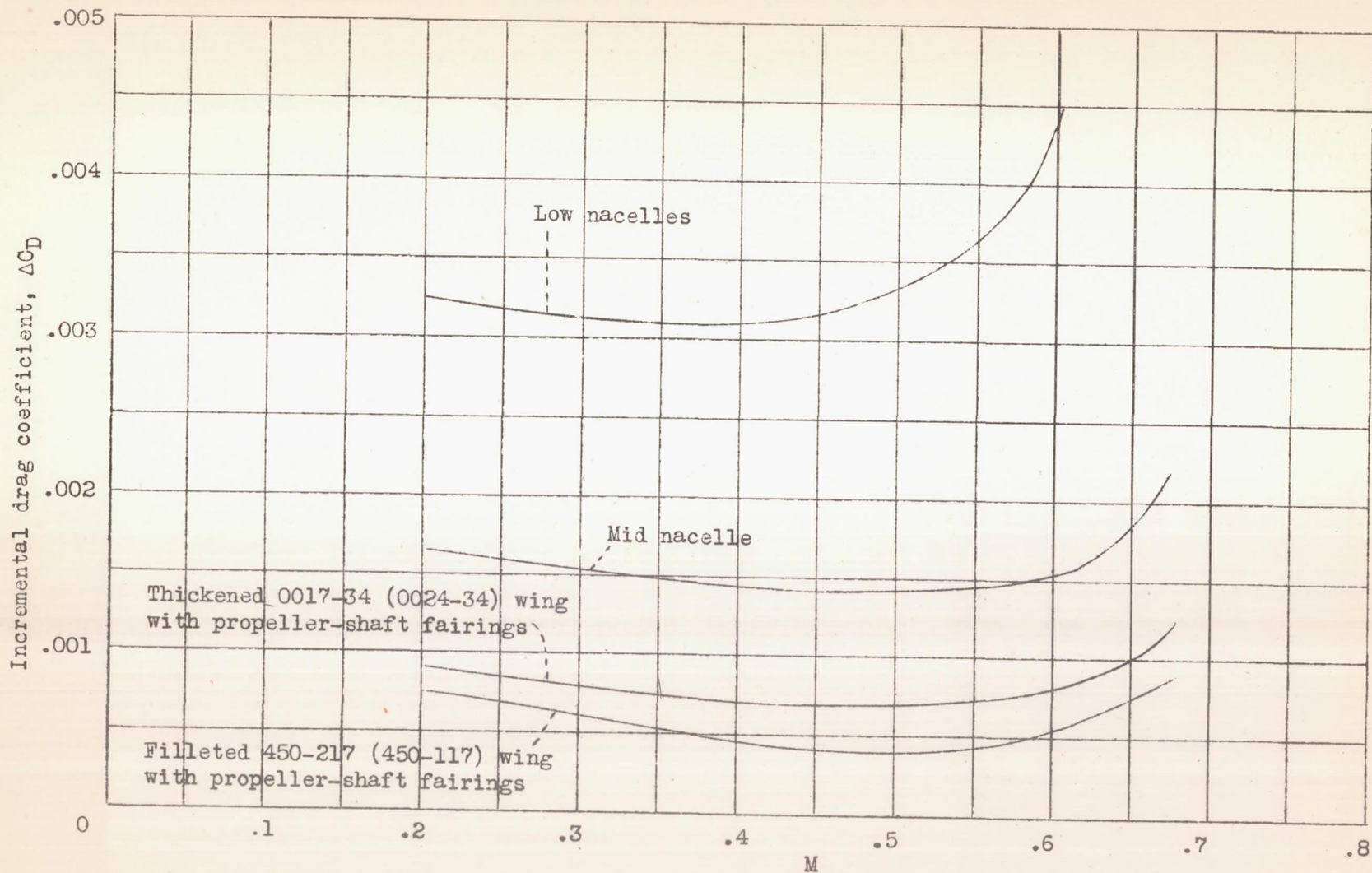Figure 5.- Incremental drag characteristics of thickened wings, propeller-shaft fairings, and nacelles. $C_L = 0.10$.

Fig. 5

Figure 6.- Incremental drag characteristics representing several engine installations. $C_L = 0.10$.

Fig. 6
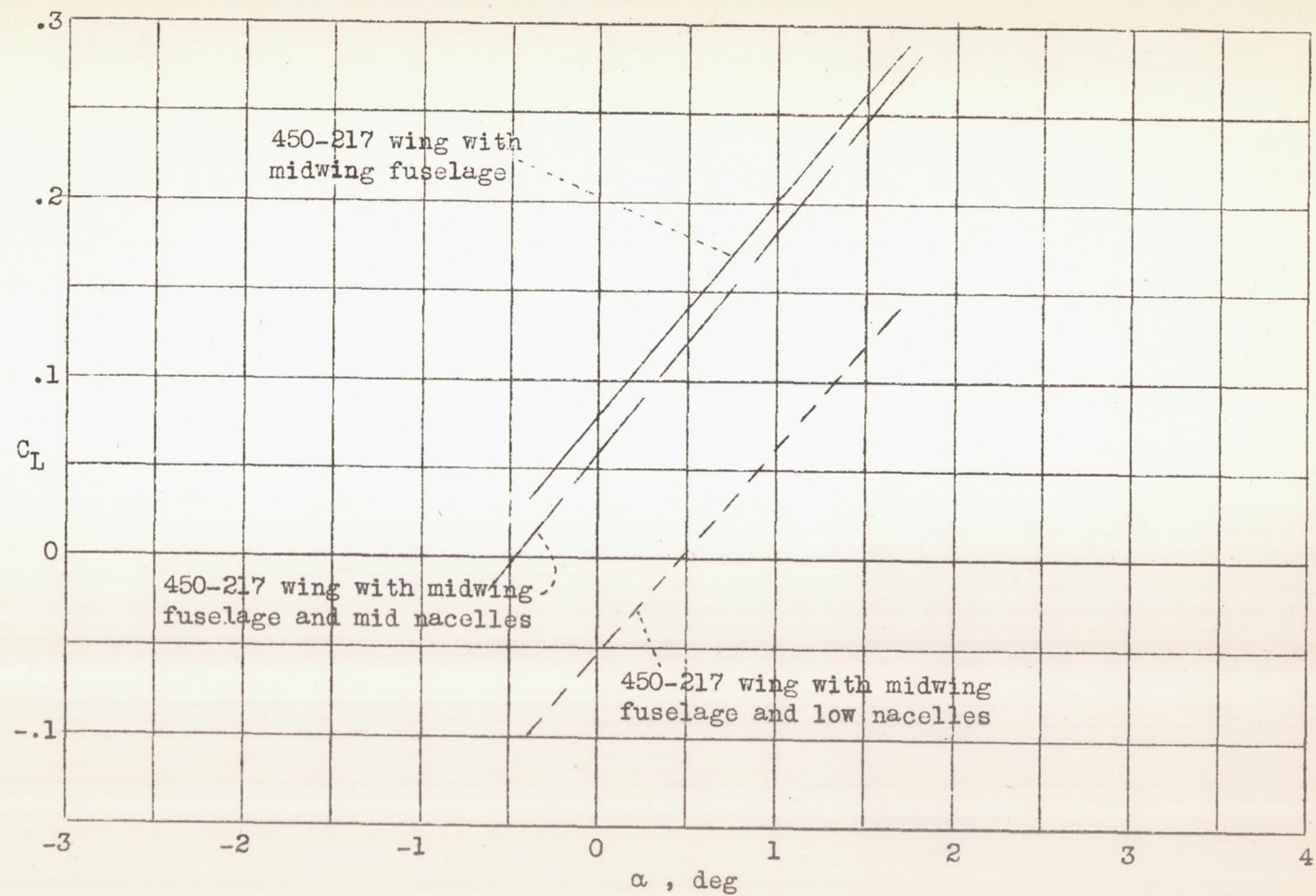
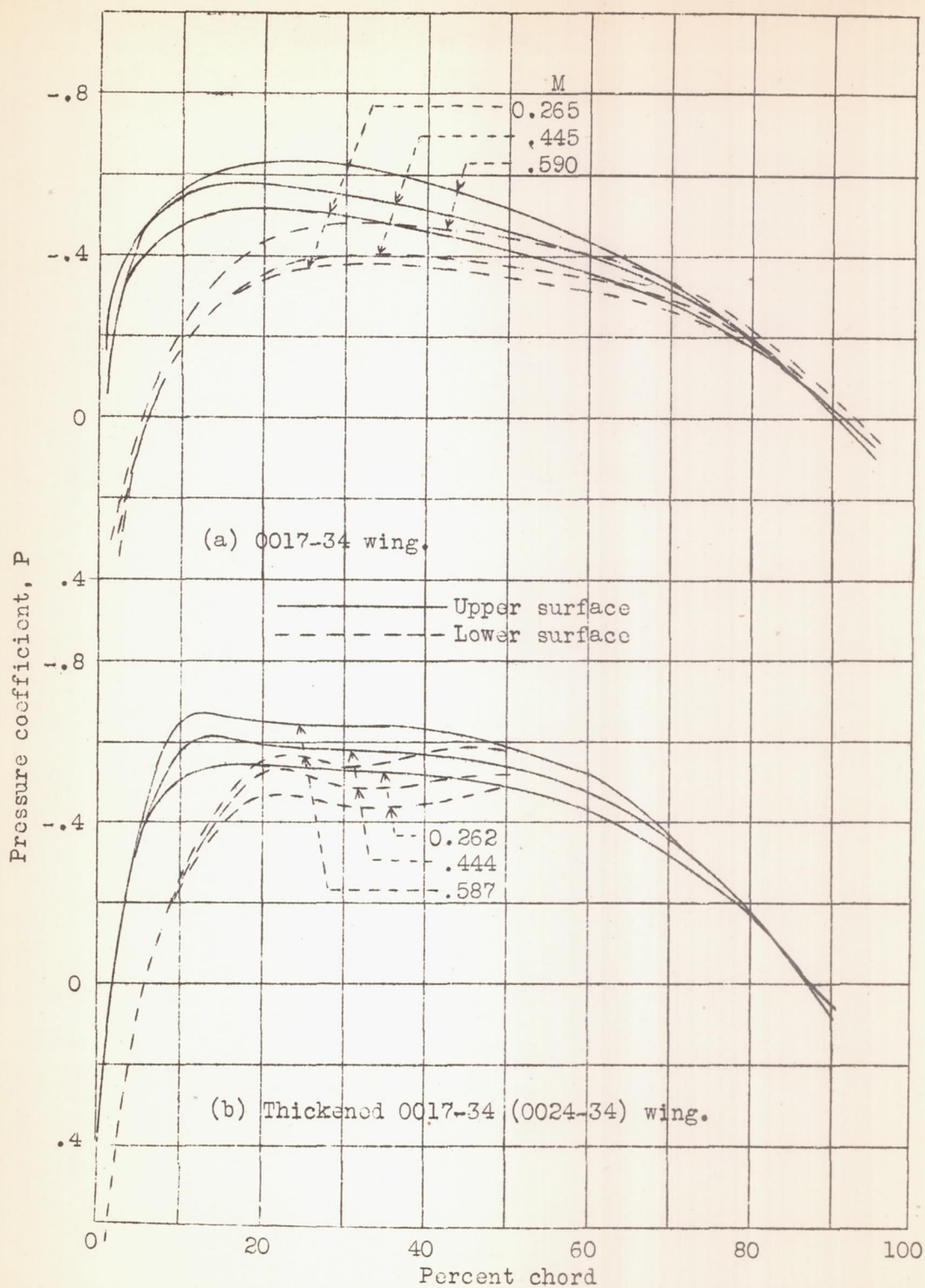Figure 7.- Effect of nacelles on lift coefficient. M = 0.50.

Fig. 7

Figure 8 (a to f).- Pressure distribution at various wing-fuselage
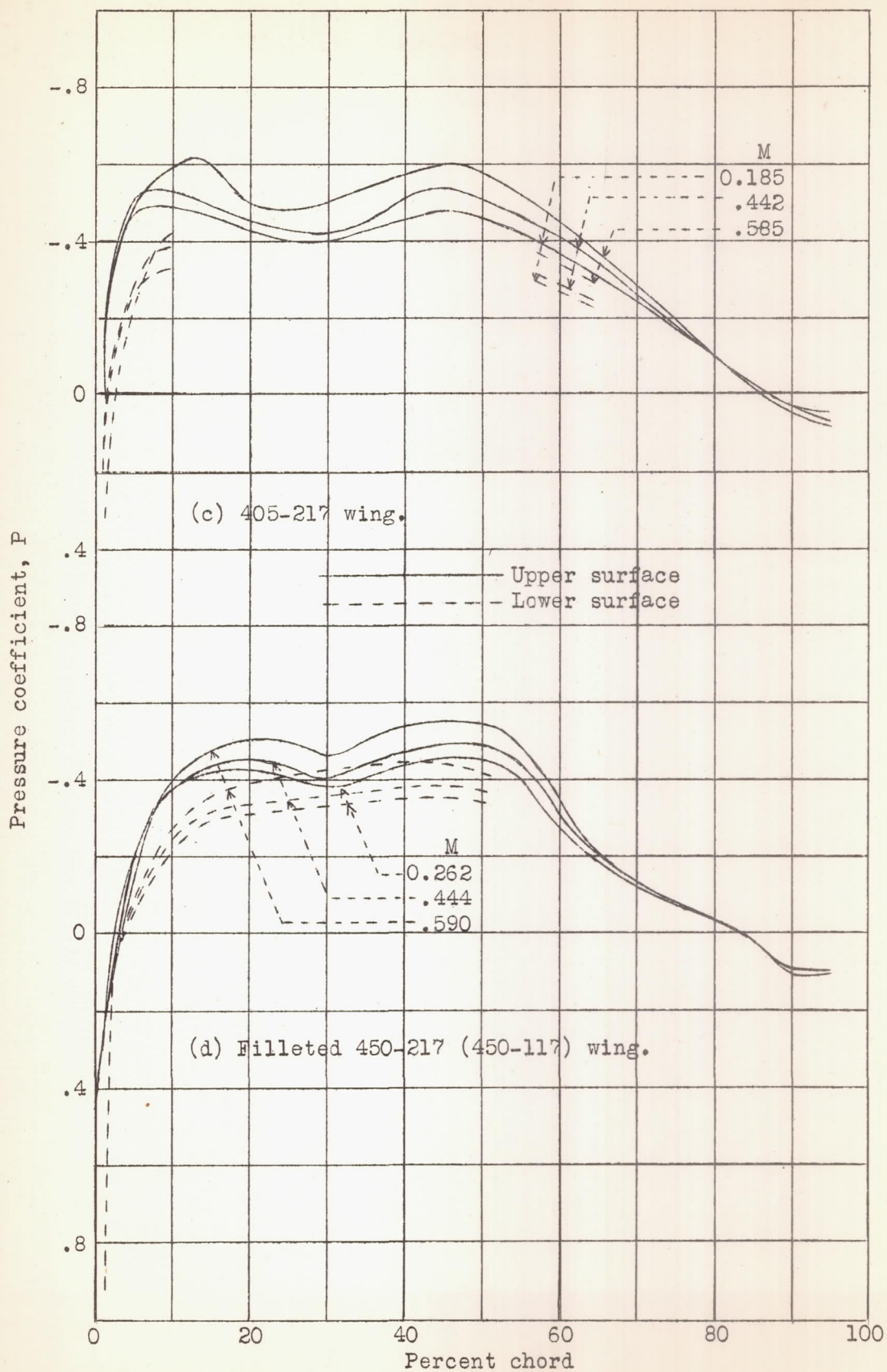juncturos. $C_L = 0.10$.

(c) 405-217 wing.

(d) Filleted 450-217 (450-117) wing.

Figure 8,- Continued.

(e) 450-217 wing with mid nacelles.
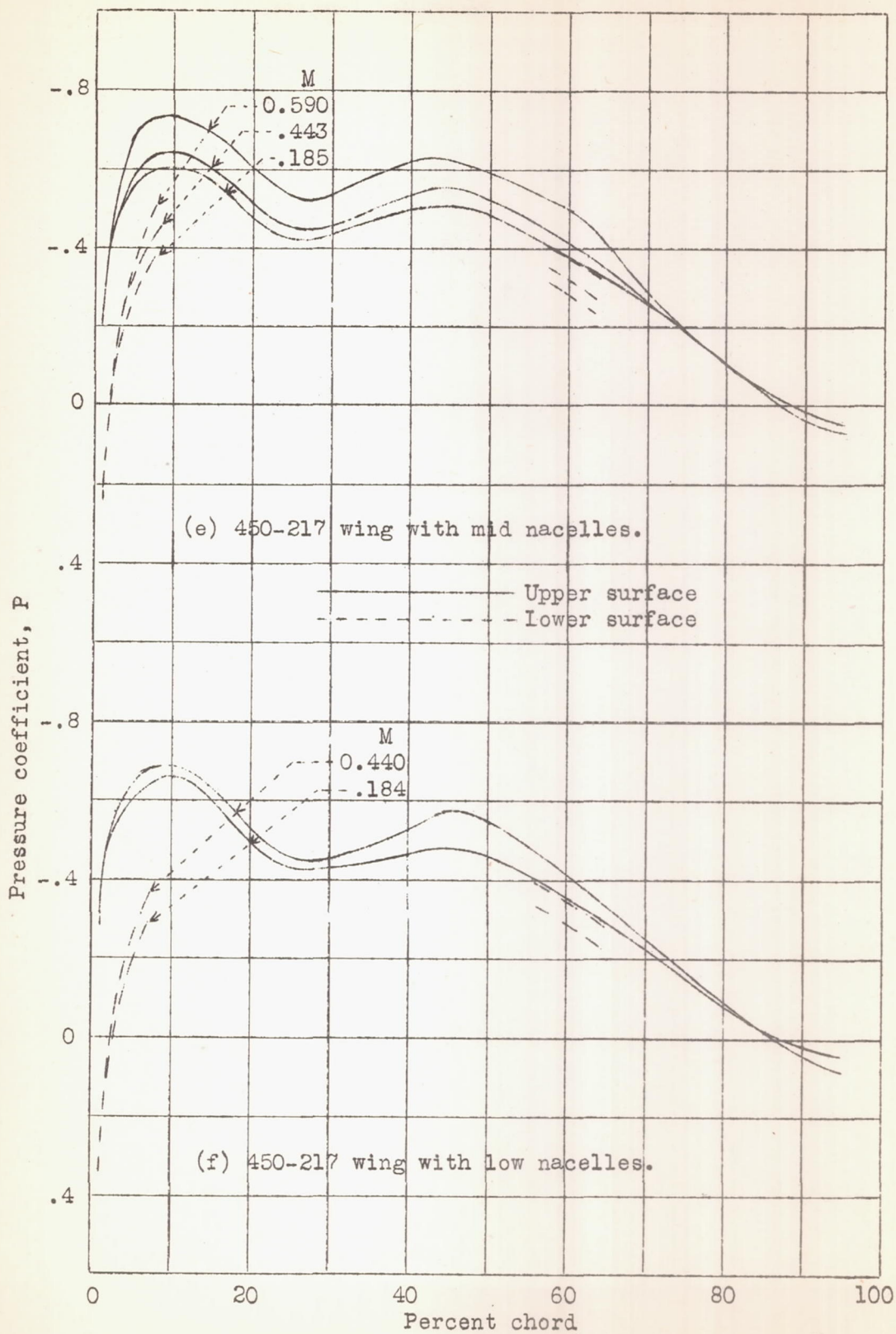
(f) 450-217 wing with low nacelles.
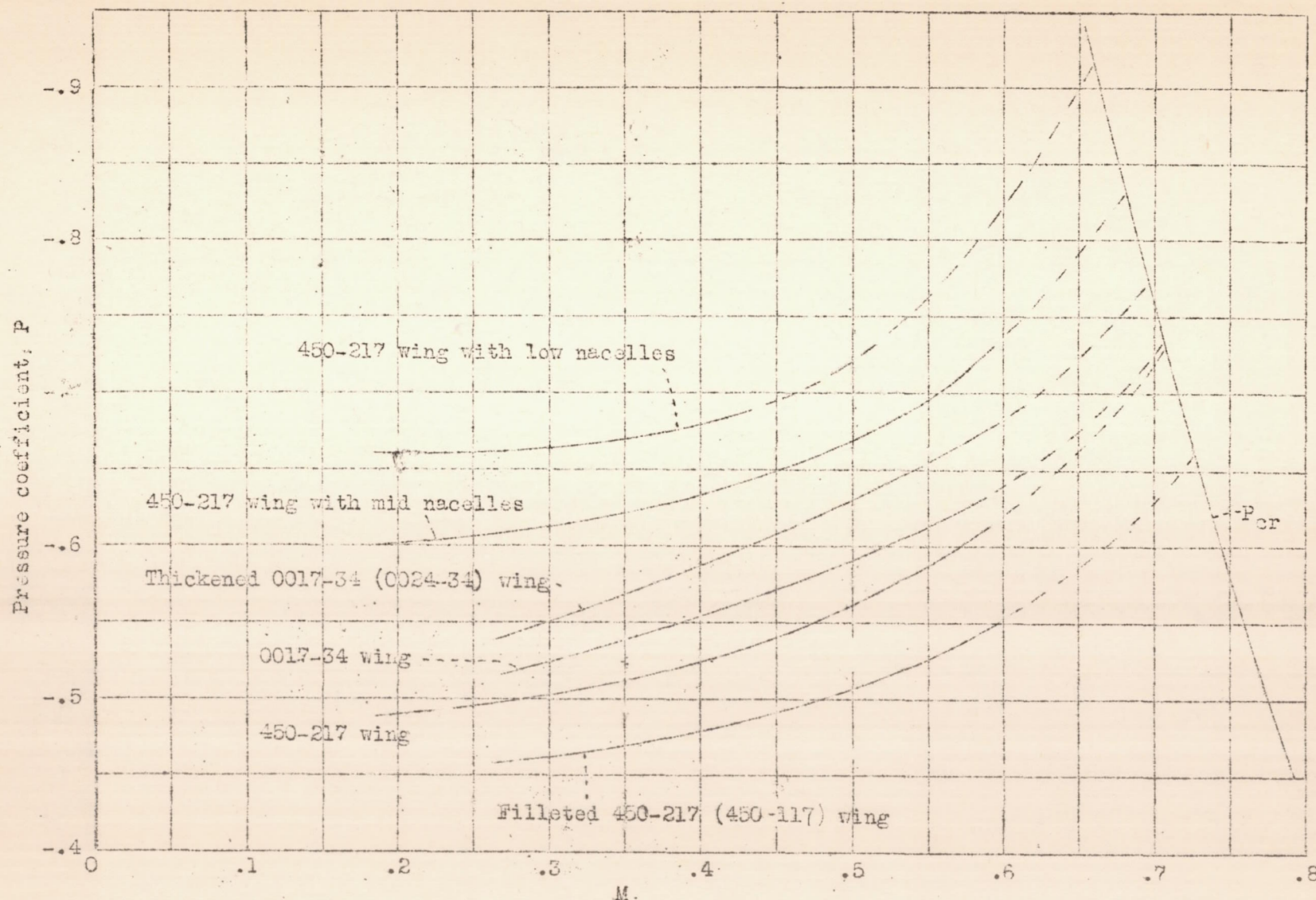
Figure 8.- Concluded.

Figure 9.- Variation of peak pressure coefficient with Mach number for various wing-fuselage junctures. $C_L = 0.10$.

Fig. 9